 doi:10.20944/preprints202211.0081.v1

Article

Influence of Reinforcing Efficiency of Clay on the Mechanical Properties of Poly(butylene terephthalate) Nanocomposite

Maria A. S. Colombo[1], Francisco R. V. Díaz[2], Deepa Kodali[3,*], Vijaya Rangari[4], Olgun Güven[5], Esperidiana A. B. Moura[1,*]

[1] Instituto de Pesquisas Energeticas e Nucleares, Centro de Quimica e Meio Ambiente, 2242 Prof. L. Prestes Av., 05508-000, Sao Paulo, SP, Brazil, mascolombo@yahoo.com.br
[2] Universidade de São Paulo, Escola Politécnica, Dep. de Eng. Metalúrgica e de Materiais, 2463 Prof. Mello de Morais, Av. 05508-900, Sao Paulo, SP, Brazil, frrvdiaz@usp.br
[3] Christian Brothers University, 650 E Pkwy South, Memphis, TN 38104, USA, dkodali@cbu.edu
[4] Department of Materials Science and Engineering, Tuskegee University, Tuskegee, AL 36088, USA, vrangari@tuskegee.edu
[5] Hacettepe University, Department of Chemistry, Polymer Chemistry Division, 06800, Beytepe, Ankara, Turkey, guven@hacettepe.edu.tr
* Correspondence: E. A. B. M.: eabmoura@ipen.br; D.K: dkodali@cbu.edu

Abstract: In contrast to the traditional fillers, clay, in particular, natural smectite clay represents an environmentally significant alternative to improve the properties of polymers. Compared to conventional nanofillers, smectite clay can effectively enhance the physical and mechanical properties of polymer nanocomposites with a relatively small amount of addition (< 5 wt%). The present study focuses on investigating the reinforcing efficiency of different amounts (up to 5 wt%) of a natural Brazilian smectite clay on the mechanical and thermal properties of poly(butylene terephthalate) (PBT) nanocomposites. Natural Brazilian clay modified by addition of quaternary salt and sodium carbonate (MBClay) was infused into the PBT polymer by melt extrusion, using a twin-screw extruder. It was found that the best properties for PBT were obtained at 3.7 wt% of modified BClay. Tensile strength at break exhibited an increase of about 60 %, flexural strength increased by 24 % and flexural modulus increased by 17 %. In addition, an increase in the crystallinity percentage of PBT/BClay nanocomposite was confirmed by DSC and XRD analysis, and a gain of about 45 % in HDT was successfully achieved due to incorporation of 3.7 wt% of MBClay.

Keywords: clay; polymer-matrix; nanocomposites; mechanical properties; morphology

1. Introduction

Despite the widespread examination of polymer/clay nanocomposites for a long time, there is an increased focus on developing naturally occurring nanoparticles such as clays, as reinforcement polymerics. The current challenge to reduce the environmental impact of polymeric nanocomposites has geared the efforts to increase the application of polymeric nanocomposites with natural fillers [1–6]. With the growing demand of polymer composites in various industries, innovative approaches have become quintessential to developing sustainable and environmentally friendly nanocomposite materials. Thus the properties of polymeric nanocomposites reinforced with clay and other nanoparticles derived from renewable sources are currently the subject of extensive research [6–18].

Owing to their layered structure and high intercalation chemistry, smectite clays from renewable sources became an attractive substitute for conventional nanofillers in polymeric nanocomposites with desirable properties [1–3,6,19]. Aside from their environmental sustainability, large availability and low cost made smectite clays a viable alternative to conventional nano-reinforcements [1,2]. A number of semicrystalline polymer matrices, such as poly(butylene terephthalate) (PBT), when reinforced by clay, have demon-

 doi:10.20944/preprints202211.0081.v1

strated desirable characteristics for a variety of practical applications. Especially, their significant improvement in heat distortion temperature, impact strength, and modulus has gained industrial interest [20–26]. Because of its easy processability, good mechanical properties, excellent dimensional stability, high stiffness, and hardness, PBT has been a highly desirable engineering thermoplastic for injection molding. PBT has been widely utilized in various applications, such as insulator in electrical and electronic industries [20–26]. Its superior thermal and mechanical properties, and excellent behavior in micromolding processes, 3D printing and additive manufacturing have increased the use of PBT for engineering materials. Predominantly, PBT is used in the automotive industry for applications such as connectors and sensors. The combination of rigidity and solvent resistance of PBT has made it a major contributor to the personal computer connector industry [23–30].

Although PBT has good mechanical properties and thermal stability, these are still insufficient for its potential applications in a wide range of industrial fields. Thus, the incorporation of different fillers in micro and nano-size into PBT has been evaluated in order to develop high-performance PBT composite materials applicable for advanced industries [26–41]. Additionally, the incorporation of only a small amount of clay, into PBT can increase the low impact strength and heat distortion temperature, and reduce the brittleness and cost, widening the field of applicability of this polyester [24,25,30]. Positive characteristics in the end product of PBT–clay nanocomposites may include several aspects: chemical resistance, surface appearance, improved fire retardancy, electrical and thermal conductivity, and mechanical properties [23–25]. Chang et al., prepared Poly(butylene terephthalate (PBT))/clay nanocomposites by melt intercalation employing a twin-screw extruder [35]. In their study, a low-viscosity PBT (η= 0.74 dL g−1) and a high-viscosity PBT (η= 1.48 dL g−1) were used. The authors observed that the PBTs may be intercalated into the organoclay, with the intercalation occurring, more extensively, for the PBT matrix with high viscosity. The results showed that clay addition caused a considerable increase in the mechanical and dynamic mechanical properties, raising the PBT non-isothermal crystallization rates. Oburoğlu et al., studied the melt-crystallization behavior of poly(butylene terephthalate) (PBT) composites with 5 wt% of fillers using commercial grades of calcite, halloysite, and organo-montmorillonite [36]. According to their results, the production rate of the injection molded parts could be significantly reduced when organically modified alumina-silicate layers are added to PBT-based composites.

The present study focuses on developing Brazilian smectite clay infused PBT nanocomposites. The contribution of this work is to provide additional insight into the reinforcing efficiency of the incorporation of different amounts (up to 5 wt%) of a natural Brazilian smectite clay on the mechanical and thermal properties of poly(butylene terephthalate) (PBT) nanocomposites prepared by melting blending in a twin-screw extruder.

2. Materials and Methods

2.1. Materials

The materials used in this study were PBT resin (Celanex 1600A- commercial grade by Celanese Corporation) with MFI = 6.5 g/10 min at 190 ^{0}C/2.16 Kg (ASTM D1238), specific density =1.31 g/cm^3, and natural brazilian smectite clay denominated Brazilian chocolate clay (BClay), from Boa-Vista, PB, Brazil.

2.2. Clay Preparation

Brazilian chocolate clay (BClay) is a smectite clay (2:1 layered silicates) polycationic with calcium ions (Ca^{2+}) occupying, predominantly, the interlayer space. The as-received BClay was modified by the addition of quaternary ammonium salt and sodium carbonate, as a source of Na^+ ions, to replace the Ca^{2+} ions [42,43]. Firstly, the clay was dispersed in deionized water (4 wt% of clay) and Na_2CO_3, at a concentration of 100 meq/100 g of clay, and was slowly added to the suspension. Then, the suspension was stirred for about 30

Preprints (www.preprints.org) | NOT PEER-REVIEWED | Posted: 4 November 2022 doi:10.20944/preprints202211.0081.v1

min, at 97°C. After that, an aqueous solution of quaternary ammonium salt was added to the suspension containing sodium smectite clay (chocolate clay-Na), at a concentration equivalent to 1.1 CEC (cation exchange capacity) of the sodium clay. After stirring for 30 min, at room temperature, the suspension was filtered and washed with deionized water. The organophilic clay (MBClay) was then dried at 60 ºC for 48 h, ground, stored at room temperature and, finally, characterized. The experimental details of the clay preparation are described in Paiva et al. and Delbem et al. [42,43]. A schematic of the clay preparation is illustrated in Scheme 1.

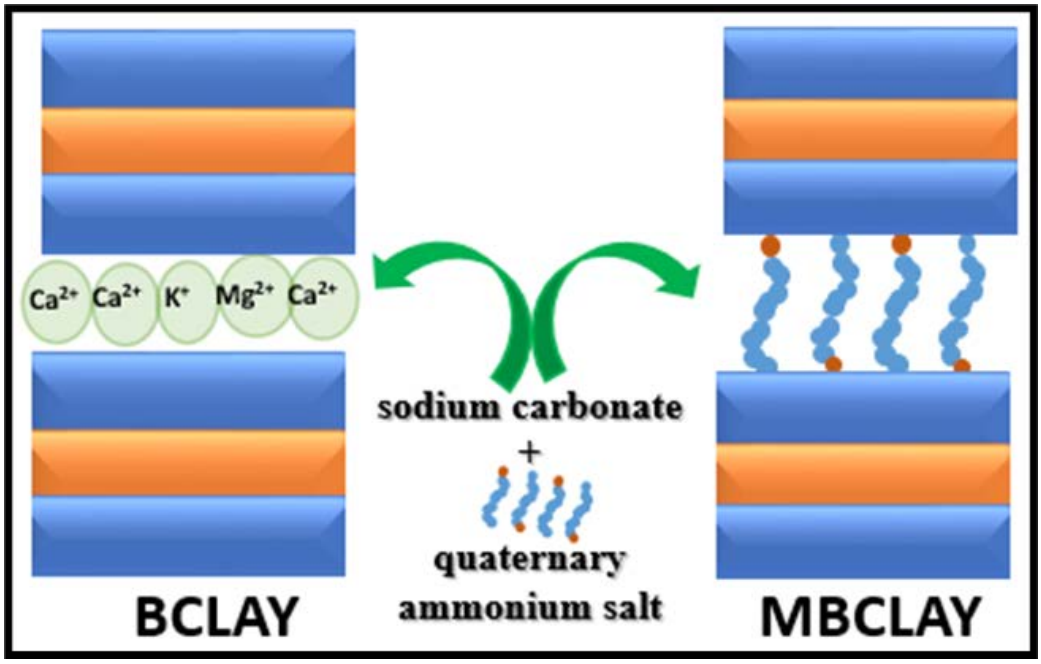

Scheme 1. Clay preparation process.

2.3. Moisture Content of Samples

Moisture in a plastic material can cause several undesirable effects, such as processing problems, poor mechanical properties or visual defects in injected parts. In order to prevent moisture causing problems in the PBT/MBClay nanocomposite, the neat PBT and MBClay were kept in a laboratory oven at 100°C before being processed. Moisture content was measured using a Mettler Toledo HR83 moisture analyzer. The moisture content in neat PBAT and BClay samples was measured for as received samples and for the samples after 4 hours of drying in the laboratory oven. Since the PBT manufacturer recommends that the moisture content of the PBT for processing to be bow 0.02%, samples with moisture content of 0.01% were considered suitable for processing [44].

2.4. Nanocomposite Preparation

PBT/MBClay nanocomposites containing different amounts (up to 5 wt%) of modified Brazilian chocolate clay (MBClay) were prepared according to compositions listed in Table 1 using a co-rotating twin-screw extruder with L/D= 25 "ZSK 18 Megalab" made by Coperion Werner & Pfleiderer GmbH & Co. The temperature profile was 200/215/220/225/230/235°C and the screw speed was 60 rpm. The resulting extrudates were cooled down for a better dimensional stability, pelletized, dried at 100 ± 2 º C, for 4 h in a circulating air oven and fed into an injection molding machine Sandreto 430/110 to obtain standard ASTM test specimens. A schematic of the nanocomposite preparation is illustrated in Scheme 2.

Preprints (www.preprints.org) | NOT PEER-REVIEWED | Posted: 4 November 2022 doi:10.20944/preprints202211.0081.v1

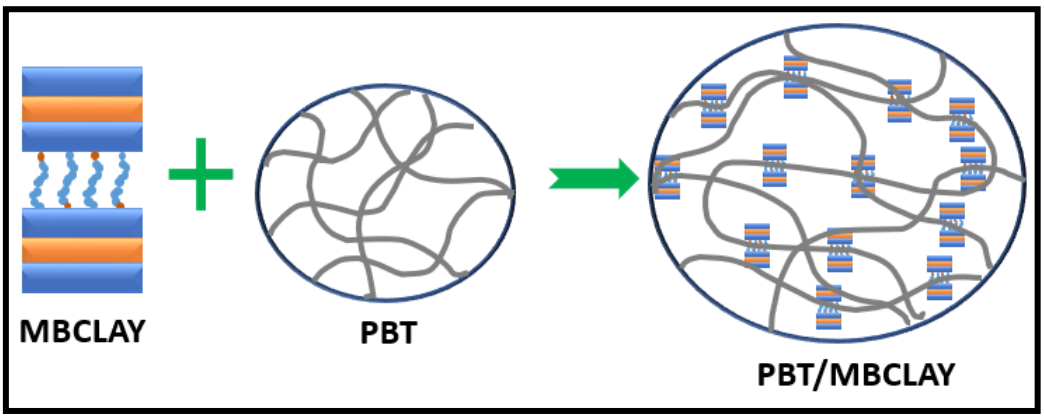

Scheme 2. Schematic of nanocomposite preparation.

Table 1. Nanocomposites composition.

Samples	PBT (%wt)	MBClay (%wt)
Neat PBT	100	0
PBT/MBClay 3.0%	97.0	3.0
PBT/MBClay 5.0%	95.0	5.0

2.5. Characterization of Brazilian Clay

2.5.1. Measured clay content

The measurement of clay content in PBT matrix was performed using a muffle furnace according to ASTM D – 5630 standards. A sample of 10g of each PBT/MBClay formulation obtained from extrusion process was weighed, placed in crucibles, taken to the muffle furnace and heated to 600°C for one hour, until the material was completely incinerated. To extract the clay content of each PBT/MBClay formulation, the porcelain crucibles containing the clay content were weighed again after the material was completely burned and cooled. The percentage of clay content in each PBT/MBClay formulation was calculated by equation (1)

$$X_{MBClay}(\%) = 100 - \frac{WI_{Sample} - WF_{Sample}}{WI_{Sample}} \times 100 \quad (1)$$

where X_{MBClay} (%) is percentage of clay content in each PBT/MBClay formulation; WI_{Sample} is initial weight of sample (weight of porcelain crucibles with PBT/MBClay), WF_{Sample} is final weight of sample (weight of porcelain crucibles with burned material).

2.5.2. X-Ray Diffraction (XRD) of Clay

The interlayer distance of the natural and modified BClay was determined by XRD. The XRD patterns of natural and modified (MBClay) were recorded on a Simens - D5000 diffractometer operated at 40 kV and 40 mA, with CuKα radiation (λ = 1.54 Å), with 2θ varying between 2° to 35°. Bragg's equation (equation (2)) was used to determine the interlayer distance in crystal of the natural and MBClay:

$$d = \frac{\lambda}{2sin\theta} \quad (2)$$

where d is the distance between atomic layers in crystals; λ is wavelength of beam of X-Ray; θ is characteristic diffraction peak of MBClay.

Preprints (www.preprints.org) | NOT PEER-REVIEWED | Posted: 4 November 2022 doi:10.20944/preprints202211.0081.v1

2.5.3. Transmission Electron Microscopy (TEM)

TEM analysis of natural and MBClay was performed using a JEOL-2010 TEM. Natural and modified BClays were dispersed in ethanol solution and then a drop of the solution was distributed on copper grid which was analyzed in TEM with an operating voltage of 80 kV.

2.6. Characterization of Neat PBT and PBT/MBClay Nanocomposites

2.6.1. X-Ray Diffraction (XRD) of composites

The XRD analysis of neat PBT and PBT/MBClay nanocomposites was performed using a Rigaku-Denki MultiFlex diffractometer (Rigaku Denki Co. Ltd.) with CuKα radiation (λ = 1.5406 Å) at 40 kV and 20mA, with 2θ varying between 2° to 35°.

2.6.2. Microscopy Analysis of Composites

The scanning electron microscopy (SEM) of cryofractured neat PBT and PBT/MBClay sample surfaces was performed using LX 30 (Philips) instrument. The fractured surface of the sample was coated with a fine layer of gold prior to observation.

A small sample was microtomed using a Leica EM UC6 at room temperature to obtain ultra-thin PBT/MBClay specimens for TEM. The analysis of PBT/MBClay nanocomposites was performed using a JEOL-2010 TEM.

2.6.3. Differential Scanning Calorimetry (DSC)

DSC analyses of neat PBT and PBT/MBClay nanocomposites were carried out using a SDT Q 600 (TA Instruments), on four weighed samples with 5.0 ± 0.5 mg of material. Samples were heated from 25 to 300°C, at a heating rate of 10°C/min (in an oxygen atmosphere). The scans were taken from the second heating cycle to eliminate any thermal history of the samples. Crystallinity was calculated from melting peak areas. The percentage of crystallinity (χ_c) of nanocomposite material was calculated using equation (3), where ΔH_m is the melting enthalpy of the of PBT/MBClay nanocomposites. ΔH_m^o is initial melting enthalpy of the PBT assuming 100 % crystallinity which is 140 J/g, W_{PBT} is the mass fraction of the PBT in the nanocomposites; χ_c is percentage crystallinity of PBT in PBT/MBClay nanocomposites

$$\chi_c = \frac{\Delta H_m}{\Delta H_m^o \times W_{PBT}} \times 100\% \quad (3)$$

2.6.4. Thermogravimetric Analyses (TGA)

TGA of neat PBT and PBT/MBClay nanocomposites was carried out using a SDT Q 600 (TA Instruments). TG analyses of the materials were performed on three weighed samples with 5.0 ± 0.5 mg of the materials. Samples were heated from 25 to 600 ºC, at a heating rate of 10°C/min (in oxygen atmosphere).

2.6.5. Tensile Tests

The tensile tests of neat PBT and PBT/MBClay nanocomposites were conducted according to ASTM D 638 standards to obtain tensile strength, Young's modulus and elongation at break. An Instron Testing Machine model 5564 at 23 C was used. An average value of at least five specimens for each formulation were taken and recorded.

2.6.6. Flexure Tests

The fracture resistance and elasticity of materials, under stress, are evaluated by the determination of properties of flexural strength, flexural modulus, and fracture toughness. The flexural strength is the ability of a material to resist bending failure stress, and the flexural modulus is the measure of stiffness of the material to bending deformation.

 doi:10.20944/preprints202211.0081.v1

The flexural tests (three point bending) were determined according to ASTM D790, using 5 specimens with 3.2 mm thickness, 9.5 width and 165 mm length for each formulation, with an EMIC DL 2000 universal testing machine.

2.6.7. Izod Impact Tests

Izod impact strength is the measure of ability of material to absorb energy on collision. Notched Izod impact tests of neat PBT and PBT/MBClay were performed according to ASTM D 256 with a Ceast Resil impact tester. At least five specimens were tested for each formulation and the average values were taken.

2.6.8. Heat Distortion Temperature Tests

HDT of a polymeric material is a measure of a polymer's resistance to distortion under a given load at elevated temperature. That is, HDT values represent the upper limit of the dimensional stability of polymers in service without significant physical deformations under a given load at elevated temperature. HDT tests of neat PBT and PBT/MBClay were performed according to ASTM D 648. The mean values of at least five specimens were reported.

2.6.9. Clay's Reinforcing Efficiency

To achieve good mechanical properties, several studies indicate that clay nanocomposites like other nanocomposites need to exhibit good dispersion, exfoliation, surface compatibilization and also good stress transfer between the clay and the polymer matrix. The existence of agglomerations significantly reduces the effective aspect ratios of clay, causing stress concentration phenomenon and preventing efficient load transfer from the reinforcing phase to the polymer matrix phase, and consequently reducing the mechanical properties of clay nanocomposites. Therefore, the reinforcing efficiency of MBClay on the mechanical properties of PBM/MBClay nanocomposites depends more specifically on clay dispersion and exfoliation, and the presence of agglomerations than on the MBClay content. In order to quantify the reinforcing efficiency of the MBClay on the PBM/MBClay nanocomposites, the mechanical properties of nanocomposites were normalized by being divided by the corresponding mechanical properties of the neat PBT as shown in equation (4):

$$Reinforcing\ efficiency\ (\%) = \frac{M_N - M_{PBT}}{M_{PBT}} \times 100 \quad (4)$$

3. Results and Discussion

3.1. Brazilian Clay Characterization Results

3.1.1. Measured Clay Content

Table 2 presents the corrected nanocomposite composition, according to the percentage of clay content in each PBT/MBClay formulation calculated by equation (1).

Table 2. Corrected nanocomposites composition.

Samples	PBT (%wt)	MBClay (%wt)
Neat PBT	100	0
PBT/MBClay 3.7%	96.3	3.7
PBT/MBClay 4.9%	95.1	4.9

Preprints (www.preprints.org) | NOT PEER-REVIEWED | Posted: 4 November 2022 doi:10.20944/preprints202211.0081.v1

3.1.2. XRD Analysis

The XRD patterns of natural and modified BClay are shown in Figure 1. XRD pattern of natural BClay shows a peak at 2θ = 6.58, which corresponds to an interlayer distance (d_{001}) of 1.34 nm. However, the pattern of modified BClay (MBClay) gives a significant peak at 2θ of 4.58 that corresponds to the d_{001} distance expanded to 1.93 nm, which suggests that the interlayer distance (d_{001}) of MBClay increased after modification. This increase confirms the intercalation of the quaternary ammonium cation in the interlamellar spacings of the MBClay. These results are also consistent with other modified clays [36,42].

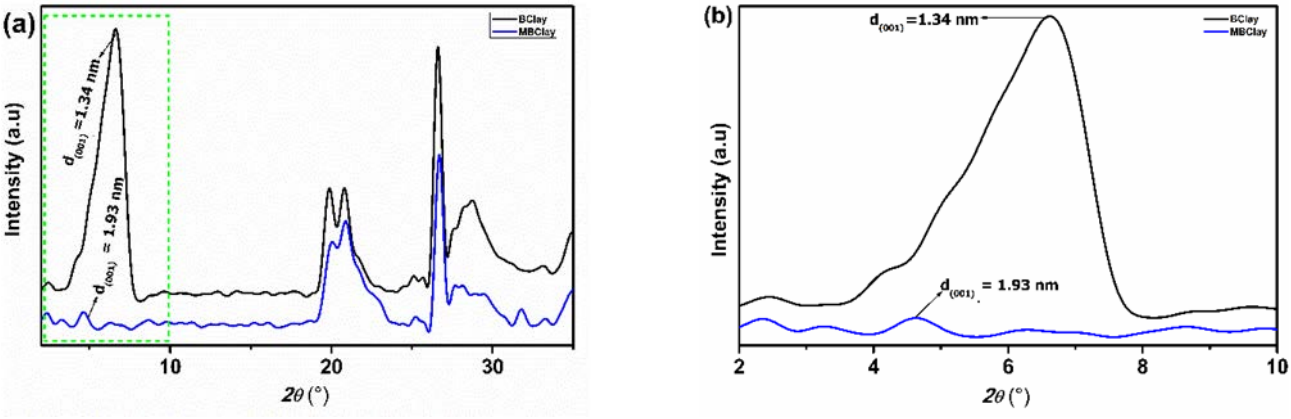

Figure 1. (a) XRD patterns of natural and modified BClay in the 2θ range from 2 to 35°; (b) expanded view of the XRD patterns in the 2θ range from 2 to 10°.

3.1.3. TEM Analysis

TEM images of natural and modified BClays are shown in Figure 2. The natural BClay shows crystalline structure with agglomerated particles and with irregular size and shapes which is shown in Figures. 2(a) and (b). Figures 2(c) and (d) show the TEM images of the modified BClay with layered crystalline structure showing homogeneous distribution of particles with reduced size, and the absence of agglomerations.

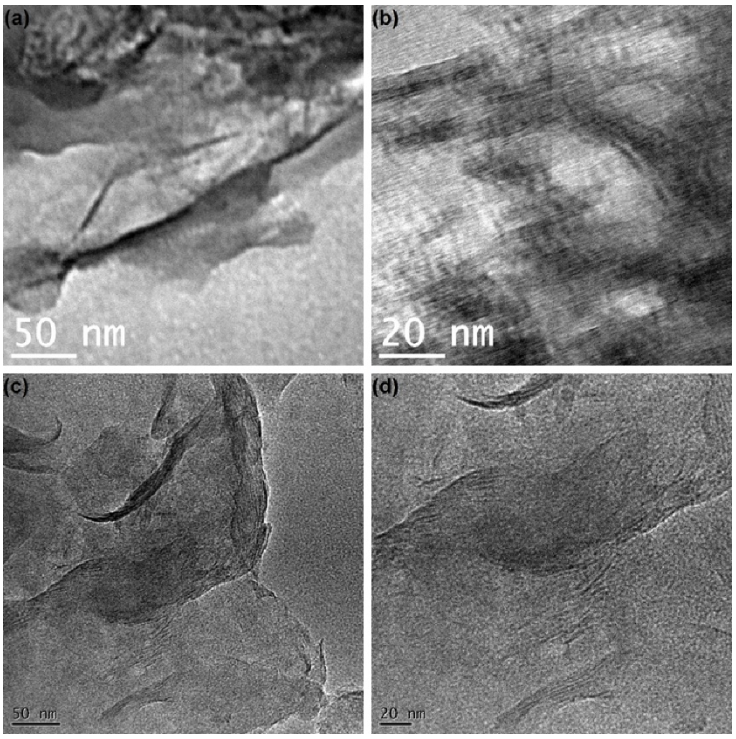

Preprints (www.preprints.org) | NOT PEER-REVIEWED | Posted: 4 November 2022 doi:10.20944/preprints202211.0081.v1

Figure 2. TEM **micrographs of** natural and modified BClay:(a) natural BClay 50 nm; (b) natural BClay 20 nm; (c) modified BClay 50 nm, and (d) modified BClay 20 nm.

3.2. PBT/MBClay Nanocomposite Analysis

3.2.1. XRD Analysis of Composites

Figure 3 shows the XRD pattern for the modified BClay (MBClay), neat PBT and PBT/BClay nanocomposites for 2θ varying between 2° and 35°. The characteristic and intense peaks for the neat PBT are observed at 2θ positions of 15.75° and 17.23°, corresponding to the β-crystallite form of PBT, and at 2θ of 20.34°, 21.41°, 23.40°, and 24.96°, corresponding to the *α*-crystallite form of PBT as shown in Figure 3(a) [44,45]. These characteristic crystalline peaks were also observed for the PBT/MBClay with 3.7– 4.9 wt% of MBClay loadings. However, their positions were slightly shifted to lower angles. In addition to that, a very small peak is observed at 2θ = 4.58° for PBT/MBClay of 3.7 wt% which is shown in highlighted area in Figure 3(a) as well as in the expanded view (Figure 3(b)).

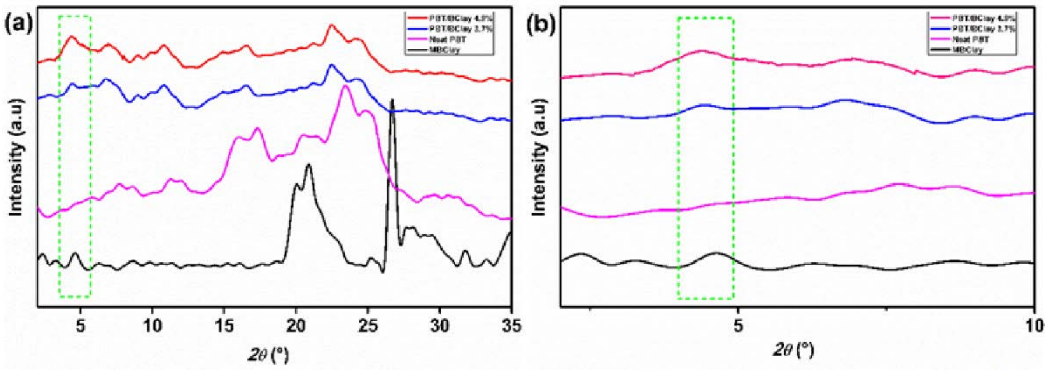

Figure 3. XRD patterns for the MBClay, neat PBT and PBT/MBClay nanocomposites: (a) in the range of 2θ between 2° to 35°; (b) in the range between 2° to 10°.

A more intense characteristic MBClay peak was observed for 4.9% MBClay loading. It is evident that a small amount of MBClay agglomerates in the PBT matrix after adding 3.7 wt% of MBClay, with the agglomeration possibly increasing after adding 4.9 wt% of MBClay. Consequently, XRD results indicate dominant exfoliation of MBClay layers and formation of intercalated structures in PBT/MBClay nanocomposite samples containing low percentages of MBClay (3.7 wt%). However, when the amount of MBClay increased to 4.9 wt%, the dispersion of MBClay in PBT matrix became difficult and the agglomerates on the matrix surface prevailed under their exfoliation. The SEM images in the later sections confirm the effects of the increased MBClay wt% incorporated into PBT matrix in the formation of agglomerates.

3.2.2. Surface Morphology of the Composites

The dispersion state of the addition of MBClay into PBT matrix was confirmed further by using the SEM and TEM. SEM micrographs of cryo-fractured surfaces of PBT and PBT/Clay nanocomposite are compared in Figure 4. As shown in Figures 4(b) and (c), PBT/Clay nanocomposite, depicts a slightly rough cryo-fractured surface, compared to neat PBT (Figure 4(a)). However, from Figure 4(b) it is clearly evident that the clay particles are uniformly dispersed in the polymer matrix, whereas Figure 4(c) shows that the clay particles are agglomerated in polymer matrix surface with the increased amount of MBClay in PBT matrix.

Preprints (www.preprints.org) | NOT PEER-REVIEWED | Posted: 4 November 2022 doi:10.20944/preprints202211.0081.v1

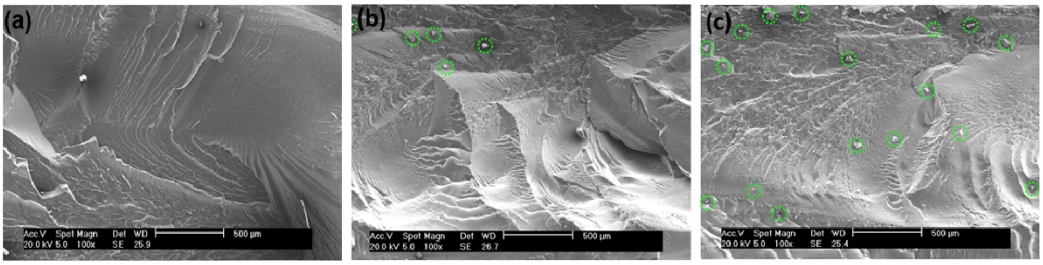

Figure 4. SEM micrographs of cryo-fractured surfaces of neat PBT and PBT/Clay nanocomposites; (a) neat PBT; (B) PBT/Clay 3.7 wt% and (c) PBT/Clay 4.9 wt%.

TEM analysis was carried out to further analyze the homogenous dispersion of the clay particles in polymer matrix surface for 3.7 wt% loading as shown in Figure 4(b). TEM micrographs of PBT/Clay nanocomposite with 3.7 wt% of MBClay were shown in Figure 5. The dark lines are the intersections of thick MBClay sheets, and the spaces between the dark lines are presumed to be interlayer spaces.

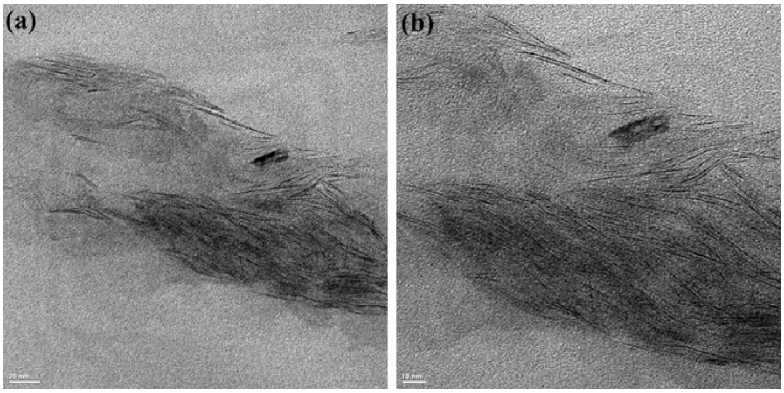

Figure 5. TEM micrographs of PBT/Clay nanocomposites content with 3.7 wt% of MBClay (a) low magnification and (b) high magnifictaion.

Some of the MBClay layers show individual dispersion of delaminated sheets in the PBT matrix. In addition to that, a region where the regular stacking arrangements is maintained with a layer of polymer between the sheets is also shown. Although a face-to-face layer morphology is retained, the layers are irregularly separated by polymer. From the results of XRD and TEM micrographs, it is clear that the morphology of PBT/Clay nanocomposites with 3.7 wt% of MBClay presents a mixture of intercalated and partially exfoliated structures. This result indicates that PBT chains have diffused into the gallery of the MBClay and the MBClay has been successfully intercalated in the PBT matrix.

3.2.3. Thermal Analysis

The melting enthalpy ΔH_m, melting temperature T_m, and crystallinity, χ_c, percentage obtained from the DSC analysis for the neat PBT and PBT/BClay nanocomposites were summarized in Table 3.

Table 3. Melting enthalpy, ΔH_m, melting temperature, T_m crystallinity, χ_c (%), onset degradation temperature and total weight loss for the neat PBT and PBT/MBClay nanocomposites.

Materials	ΔHm (J/g)	χ_c (%)	Tm (°C)	Onset Temp (°C)	Total Weight Loss (%)
Neat PBT	41.0	29.22	212.9	332.5	89.6
PBT/Clay (3.7 wt%)	45.6	34.1	213.7	331.2	83.6

 doi:10.20944/preprints202211.0081.v1

PBT/Clay (4.9 wt%)	46.1	34.6	219.1	337.2	82.5

As shown in Table 3, the melting enthalpy values of neat PBT increased to about 10 %, and the crystallinity percentage of neat PBT increased from 29.2 % to 34.6 %, with the MBClay infusion. This is attributed to the nucleation effects of clay and the improvement in the crystal perfection of PBT. A similar observation is reported by Chow, W. S. for the PBT/Montmorillonite [24].

The results of the thermogravimetric analyses (TGA), onset temperature and the total weight loss were also presented in Table 3. The results showed that there were no significant changes ($p < 0.05$) in the onset degradation temperature of PBT/BClay nanocomposite, when compared with those of neat PBT. However, the total weight loss was up to 7% less than neat PBT.

3.2.4. Tensile Test

The tensile test results for the neat PBT and PBT/ MBClay nanocomposites are shown in Table 4. There is a significant dependence of the tensile properties of PBT/MBClay nanocomposites on the MBClay content. The incorporation of very small quantity (3.7 wt%) of MBClay into PBT can substantially improve the tensile properties of PBT/MBClay nanocomposites.

Table 4. Tensile tests results for the neat PBT and PBT/MBClay nanocomposites.

Tensile Parameters	**Neat PBT**	**PBT/MBClay 3.7 wt%**	**PBT/MBClay 4.9 wt%**
Tensile stress at yield (MPa)	59.2 ± 4.1	60.6 ± 1.5	48.4 ± 1.8
Tensile strength at break (MPa)	38.0 ± 3.4	60.1 ± 1.9	47.9 ± 1.6
Young's modulus (GPa)	2.5 ± 0.1	2.7 ± 0.1	2.6 ± 0.1
Elongation at break (%)	161.6 ± 35	21.1 ± 1.0	20.5 ± 1.3

The PBT/MBClay nanocomposites with 3.7 wt% of MBClay exhibited higher tensile properties compared to neat PBT and PBT/MBClay nanocomposite with 4.9 wt% of MBClay. The tensile stress at yield, tensile strength at break, and Young's modulus of PBT/MBClay nanocomposites with 3.7 wt% of MBClay were significantly increased by 2.4%, 58.2% and 8.0%, respectively, compared to neat PBT. This can be attributed to the stiffness and nanoreinforcing effects of MBClay and also the good interfacial interaction between the MBClay and PBT matrix. The MBClay is able to act as nanoreinforcing filler due to its high aspect ratio, platelet structure, and uniform dispersion in the PBT matrix. A smaller increase effect was observed at higher MBClay content (4.9 wt%) compared to MBClay with 3.7 wt%. The improvement in the mechanical properties of PBT/MBClay nanocomposites was not increased at higher MBClay content as expected, in comparison to that of smaller MBClay content. Because of intrinsic Vander Waals attractions between individual platelets within MBClay, it is possible that they tend to group together. As a result of the high aspect ratio and large surface area, it is difficult for their dispersion in the matrix to be uniform, causing agglomerations. The agglomerations thus formed can lead to the stress concentration phenomenon, preventing efficient load transfer to the PBT matrix. The elongation at break of PBT/MBClay nanocomposites was smaller than that of neat PBT, likely due to the presence of agglomerated and intercalated MBClay layers in the PBT matrix. Similar tensile behaviors were reported by other studies [24,26,41,46].

 doi:10.20944/preprints202211.0081.v1

3.2.5. Flexural Test

The flexural test results for the neat PBT and of PBT/MBClay nanocomposites are shown in Table 5. The flexural strength and flexural modulus of PBT/MBClay nanocomposites also increased with the introduction of MBClay. This enhancement of the flexural strength and modulus were attributed to the reinforcement of PBT due to incorporation of the dispersed MBClay. The enhancing effect of the flexural properties by incorporating MBClay was more significant at low MBClay content, indicating that a low MBClay loading was more effective in improving the overall mechanical properties of PBT/MBClay nanocomposites. The high MBClay content resulted in low intercalation, poor dispersion in the PBT matrix and presence of agglomerations. From these results, it is apparent that due to the increased MBClay content, the stiffness of the PBT/MBClay nanocomposites decreases gradually under flexure loading, it means that smaller resistance to bending deformation as the content of MBClay increases. Similar results has been reported in the literature [16,24,47–50].

Table 5. Flexural tests results for the neat PBT and PBT/MBClay nanocomposites.

Tensile Parameters	Neat PBT	PBT/MBClay 3.7 wt%	PBT/MBClay 4.9 wt%
Flexural strength (MPa)	74.2 ± 3.2	91.7 ± 2.8	78.7 ± 3.6
Flexural modulus (GPa)	2.4 ± 0.2	2.8 ± 0.1	2.5 ± 0.7

3.2.6. Izod Impact Test

Unlike the tensile and flexural test results, the notched Izod impact results of PBT presented a large decrease with increasing MBClay content, with PBT/MBClay nanocomposites having the lowest impact strength of 47.2 J/m, ca. 35 % lower than neat PBT, for MBClay with 3.7 wt%. The Izod impact strength of PBT/MBClay nanocomposites with 4.9 wt% of MBClay was observed to be 37.4 J/m, ca. 48.5 % lower than neat PBT. Izod impact test results of neat PBT and PBT/MBClay are presented in Table 6. This could be attributed to the presence of MBClay agglomerates which acted as stress concentrators and initiated crack propagations in the PBT matrix. At higher MBClay content, the agglomeration became more significant and thus, further lowering the impact strength. It can be seen that the Izod impact strength has similar trend to elongation at break, where the addition of MBClay caused their reduction. The low elongation at break shows that area-under-the-curve value in stress-strain curve is small indicating that the PBM/MBClay nanocomposites have small capability to absorb energy. This result was consistent with other studies [3,34,41,51,52].

Table 5. Izod impact and HDT tests results for the neat PBT and PBT/MBClay nanocomposites.

Test	Neat PBT	PBT/MBClay 3.7 wt%	PBT/MBClay 4.9 wt%
Izod Impact (J/m)	72.6 ±2.1	47.2 ± 1.4	37.4 ± 1.1
HDT (1.82 MPa) (°C)	55.4 ± 3.2	80.1 ± 6.2	69.7 ± 5.3

3.2.7. Heat Distortion Temperature

HDT test results of neat PBT and PBT/MBClay are presented in Table 6. As shown in this Table, the HDT values of PBT/MBClay nanocomposites increased with increasing MBClay content. The increasing effect of the HDT value by incorporating MBClay was more significant at low MBClay content (3.7 wt%) than at high content (4.9 wt%), because

Preprints (www.preprints.org) | NOT PEER-REVIEWED | Posted: 4 November 2022 doi:10.20944/preprints202211.0081.v1

of the dispersion of clay particles, the higher degree of crystallinity, intercalation, and low presence of agglomerations.

The HDT values of PBT/MBClay nanocomposites increased with increasing MBClay content. The increasing effect of the HDT value by incorporating MBClay was more significant at low MBClay content than at high content. The results showed that neat PBT has HDT value of about 55.4°C (HDT, 1.82 MPa), while for the nanocomposite with 3.7 wt% of MBClay has the HDT value of about 80.1°C , and for the composite with 4.9 wt% of MBClay, the HDT value was about 69.7°C . This behavior of HDT is due to the better dispersion and intercalation of clay particles, the low presence of agglomerations, and the higher crystallinity degree of nanocomposite at low MBClay content. According to the previous studies conducted by other researchers, the variation of the HDT value is closely related to the behavior of flexural modulus and onset temperature of the degradation with good dispersion of incorporated clay [2,16,22,47,50].

3.2.8. MBClay's Reinforcing Efficiency

The variations of the reinforcing efficiency of MBClay on mechanical properties of PBT/MBClay nanocomposites are shown in Figure 6. The reinforcement of 3.7 wt% of MBClay resulted in reinforcing efficiency of 58.2% at tensile strength at break whereas for 4.9 wt% of MBClay, the reinforcing efficiency at tensile strength at break was only 26.1 %. Likewise, the reinforcing efficiency of 3.7 wt% MBClay at Young's modulus was 8 %, flexural strength was 23.6 % and flexural modulus was 16.7 %. The addition of 4.9 wt% of MBClay led to the reinforcing efficiency of only 4.0 % in Young's modulus, 6.1 % in flexural strength and 4.2 % in flexural modulus of PBT/MBClay nanocomposites. Therefore, as shown in Figure 6, the effect of MBClay incorporation on the mechanical properties of PBT/MBClay nanocomposites was more significant at low MBClay content than at high content, indicating that a low MBClay loading was more effective in improving the overall mechanical properties of PBT nanocomposites.

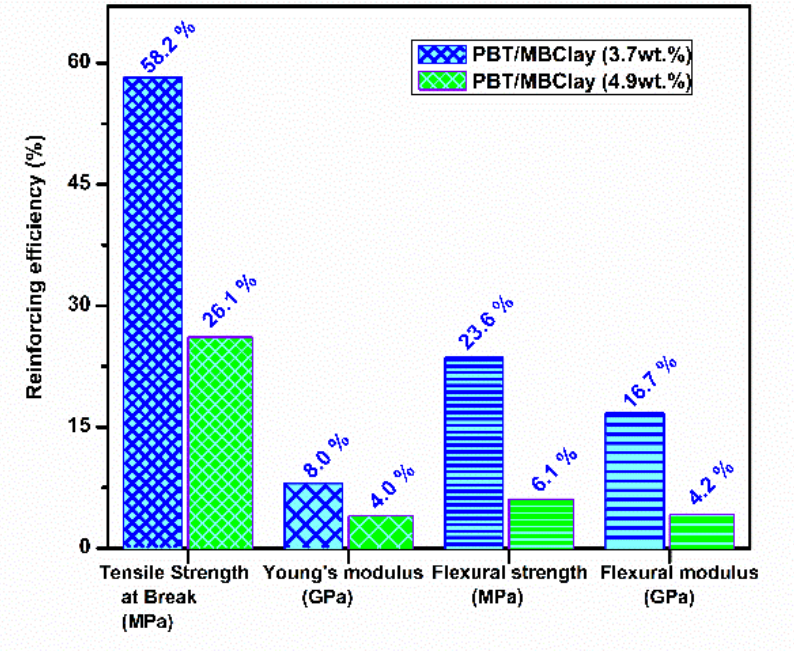

Figure 6. Reinforcing efficiency of MBClay on the mechanical properties of PBT/MBClay nanocomposites.

According to this result, it can be concluded that the incorporation of a small amount of MBClay into the PBT matrix is more effective in increasing the overall mechanical properties of PBT nanocomposites because of the high nanoreinforcing effect of MBClay, and

their uniform dispersion in the PBT matrix at a lower concentration. Hence, it is necessary to ensure good dispersion and stress transfer, to obtain high modulus and strength in the PBT/MBClay nanocomposites.

4. Conclusions

The present study focuses on the correlation between processing conditions and thermo-mechanical properties of PBT nanocomposites containing MBClay, naturally occurring smectite nanoclay, infused into the PBT matrix by extrusion processing. TEM and XRD results suggested the formation of intercalated and exfoliated structures of PBT/MBClay nanocomposites. The incorporation of only a few amounts of MBClay (up to 5 wt%) represented a significant gain in tensile strength at break, Young's modulus, flexural strength, flexural modulus, heat distortion temperature (HDT), and crystallinity of PBT. The effect of MBClay incorporation into the PBT matrix was more effective at low MBClay content (3.7 wt%) compared to high content (4.9 wt%). Under the processing conditions applied in this study, MBClay exhibited high nanoreinforcing properties and achieved uniform dispersion in PBT matrix due to its stiffness and high nanoreinforcing effect.

Author Contributions: Investigation, data curation, M. A. S. C.; methodology, supervision, formal analysis, F. R. V. D.; supervision, validation, writing - review & editing, D. K.; methodology, conceptualization, funding acquisition, supervision, V. R.; methodology, conceptualization, supervision, validation, O. G.; conceptualization, formal analysis, supervision, funding acquisition, project administration, writing - review & editing, E.A.B.M.

Funding: This research was funded by Fundação de Apoio à Pesquisa do Estado de São Paulo (FAPESP), grant number: process number 2019/00862-9 and the US-National Science Foundation for financial support through NSF-CREST#1137681.

Conflicts of Interest: "The authors declare no conflict of interest

References

1. Guo, F.; Aryana, S.; Han, Y.; Jiao, Y. A Review of the Synthesis and Applications of Polymer-Nanoclay Composites. *Appl. Sci.* **2018**, *8*, 1–29, doi:10.3390/app8091696.
2. Kotal, M.; Bhowmick, A.K. Polymer Nanocomposites from Modified Clays: Recent Advances and Challenges. *Prog. Polym. Sci.* **2015**, *51*, 127–187, doi:10.1016/j.progpolymsci.2015.10.001.
3. Ali, F.; Ullah, H.; Ali, Z.; Rahim, F.; Khan, F.; Ur Rehman, Z. Polymer-Clay Nanocomposites, Preparations and Current Applications: A Review. *Curr. Nanomater.* **2016**, *1*, 83–95, doi:10.2174/2405461501666160625080118.
4. Xu, P.; Erdem, T.; Eiser, E. A Simple Approach to Prepare Self-Assembled, Nacre-Inspired Clay/Polymer Nanocomposites. *Soft Matter* **2020**, *16*, 5497–5505, doi:10.1039/c9sm01585j.
5. Ummartyotin, S.; Bunnak, N.; Manuspiya, H. A Comprehensive Review on Modified Clay Based Composite for Energy Based Materials. *Renew. Sustain. Energy Rev.* **2016**, *61*, 466–472, doi:https://doi.org/10.1016/j.rser.2016.04.022.
6. Kodali, D.; Uddin, M.J.; Moura, E.A.B.; Rangari, V.K. Mechanical and Thermal Properties of Modified Georgian and Brazilian Clay Infused Biobased Epoxy Nanocomposites. *Mater. Chem. Phys.* **2021**, *257*, 123821, doi:10.1016/j.matchemphys.2020.123821.
7. Griffin, S.; Masood, M.I.; Nasim, M.J.; Sarfraz, M.; Ebokaiwe, A.P.; Schäfer, K.H.; Keck, C.M.; Jacob, C. Natural Nanoparticles: A Particular Matter Inspired by Nature. *Antioxidants* **2018**, *7*, doi:10.3390/antiox7010003.
8. Modi, V.K.; Shrives, Y.; Sharma, A.; Sen, P.K.; Bohidar, S. Review on Green Polymer Nanocomposite AndTheir Applications. *Int. J. Innov. Res. Sci. Eng. Technol.* **2014**, *3*.
9. Hasan, K.M.F.; Horváth, P.G.; Alpár, T. Potential Natural Fiber Polymeric Nanobiocomposites: A Review. *Polymers (Basel).* 2020, *12*.
10. Ahmad, I.; Ali, F.; Rahim, F. Clay Based Nanocomposites and Their Environmental Applications. In Development and Prospective Applications of Nanoscience and Nanotechnology Nanomaterials for Environmental Applications and their Fascinating Attributes; Ahmad, I., Ali, F., Rahim, F., Eds.; Bentham Science Publisher, 2018; pp. 166–190.
11. Zazoum, B.; Triki, E.; Bachri, A. Modeling of Mechanical Properties of Clay-Reinforced Polymer Nanocomposites Using Deep Neural Network. *Materials (Basel).* **2020**, *13*, 4266, doi:10.3390/ma13194266.
12. Zare, Y.; Fasihi, M.; Rhee, K.Y. Efficiency of Stress Transfer between Polymer Matrix and Nanoplatelets in Clay/Polymer Nanocomposites. *Appl. Clay Sci.* **2017**, *143*, 265–272, doi:https://doi.org/10.1016/j.clay.2017.03.043.

13. Zare, Y. Estimation of Material and Interfacial/Interphase Properties in Clay/Polymer Nanocomposites by Yield Strength Data. *Appl. Clay Sci.* **2015**, *115*, 61–66, doi:https://doi.org/10.1016/j.clay.2015.07.021.
14. Martino, L.; Guigo, N.; van Berkel, J.G.; Sbirrazzuoli, N. Influence of Organically Modified Montmorillonite and Sepiolite Clays on the Physical Properties of Bio-Based Poly(Ethylene 2,5-Furandicarboxylate). *Compos. Part B Eng.* **2017**, *110*, 96–105, doi:https://doi.org/10.1016/j.compositesb.2016.11.008.
15. Murugesan, S.; Scheibel, T. Copolymer/Clay Nanocomposites for Biomedical Applications. *Adv. Funct. Mater.* **2020**, *30*, 1908101, doi:https://doi.org/10.1002/adfm.201908101.
16. Sinha Ray, S.; Okamoto, M. Polymer/Layered Silicate Nanocomposites: A Review from Preparation to Processing. *Prog. Polym. Sci.* **2003**, *28*, 1539–1641, doi:https://doi.org/10.1016/j.progpolymsci.2003.08.002.
17. Saleh, T.A.; Shetti, N.P.; Shanbhag, M.M.; Raghava Reddy, K.; Aminabhavi, T.M. Recent Trends in Functionalized Nanoparticles Loaded Polymeric Composites: An Energy Application. *Mater. Sci. Energy Technol.* **2020**, *3*, 515–525, doi:https://doi.org/10.1016/j.mset.2020.05.005.
18. Qasim, U.; Osman, A.I.; Al-Muhtaseb, A.H.; Farrell, C.; Al-Abri, M.; Ali, M.; Vo, D.V.N.; Jamil, F.; Rooney, D.W. Renewable Cellulosic Nanocomposites for Food Packaging to Avoid Fossil Fuel Plastic Pollution: A Review. *Environ. Chem. Lett.* **2021**, *19*, 613–641, doi:10.1007/s10311-020-01090-x.
19. Mohammed, Z.; Tcherbi-Narteh, A.; Jeelani, S. Effect of Graphene Nanoplatelets and Montmorillonite Nanoclay on Mechanical and Thermal Properties of Polymer Nanocomposites and Carbon Fiber Reinforced Composites. *SN Appl. Sci.* **2020**, *2*, 1–14, doi:10.1007/s42452-020-03780-1.
20. Pham, N.T.-H.; Nguyen, V.-T. Morphological and Mechanical Properties of Poly (Butylene Terephthalate)/High-Density Polyethylene Blends. *Adv. Mater. Sci. Eng.* **2020**, *2020*, 8890551, doi:10.1155/2020/8890551.
21. Chisholm, B.J.; Moore, R.B.; Barber, G.; Khouri, F.; Hempstead, A.; Larsen, M.; Olson, E.; Kelley, J.; Balch, G.; Caraher, J. Nanocomposites Derived from Sulfonated Poly(Butylene Terephthalate). *Macromolecules* **2002**, *35*, 5508–5516, doi:10.1021/ma012224n.
22. Wu, D.; Zhou, C.; Hong, Z.; Mao, D.; Bian, Z. Study on Rheological Behaviour of Poly(Butylene Terephthalate)/ Montmorillonite Nanocomposites. *Eur. Polym. J.* **2005**, *41*, 2199–2207, doi:10.1016/j.eurpolymj.2005.03.005.
23. Saeed, K.; Khan, I. Characterization of Clay Filled Poly (Butylene Terephthalate) Nanocomposites Prepared by Solution Blending. *Polimeros* **2015**, *25*, 591–595, doi:10.1590/0104-1428.2039.
24. Chow, W.S. Cyclic Extrusion of Poly(Butylene Terephthalate)/Organo-Montmorillonite Nanocomposites: Thermal and Mechanical Retention Properties. *J. Appl. Polym. Sci.* **2008**, *110*, 1642–1648, doi:10.1002/app.28804.
25. Heidarzadeh, N.; Rafizadeh, M.; Taromi, F.A.; Bouhendi, H. Preparation of Poly(Butylene Terephthalate)/Modified Organoclay Nanocomposite via in-Situ Polymerization: Characterization, Thermal Properties and Flame Retardancy. *High Perform. Polym.* **2012**, *24*, 589–602, doi:10.1177/0954008312446646.
26. Kalkar, A.K.; Deshpande, V.D.; Vatsaraj, B.S. Poly(Butylene Terephthalate)/Montmorillonite Nanocomposites: Effect of Montmorillonite on the Morphology, Crystalline Structure,Isothermal Crystallization Kinetics and Mechanical Properties. *Thermochim. Acta* **2013**, *568*, 74–94, doi:10.1016/j.tca.2013.06.019.
27. Yamamoto, B.E.; Trimble, A.Z.; Minei, B.; Ghasemi Nejhad, M.N. Development of Multifunctional Nanocomposites with 3-D Printing Additive Manufacturing and Low Graphene Loading. *J. Thermoplast. Compos. Mater.* **2019**, *32*, 383–408, doi:10.1177/0892705718759390.
28. Russo, P.; Cimino, F.; Acierno, D.; Lupò, G.; Petrarca, C. Poly(Butylene Terephthalate) Based Composites Containing Alumina Whiskers: Influence of Filler Functionalization on Dielectric Properties. *Int. J. Polym. Sci.* **2014**, *2014*, doi:10.1155/2014/150589.
29. Gómez, C.; Mira, J.; Carrión-Vilches, F.J.; Cavas, F. Dynamic Moduli of Polybutylene Terephthalate Glass Fiber Reinforced in High-Temperature Environments. *Materials (Basel).* **2021**, *14*, 1–13, doi:10.3390/ma14030483.
30. Cao, Y.; Xu, P.; Yang, W.; Zhu, X.; Dong, W.; Chen, M.; Du, M.; Liu, T.; Lemstra, P.J.; Ma, P. UV Resistant PBT Nanocomposites by Reactive Compatibilization and Selective Distribution of Tailor-Made Double-Shelled TiO2 Nanohybrids. *Compos. Part B Eng.* **2021**, *205*, 108510, doi:https://doi.org/10.1016/j.compositesb.2020.108510.
31. Wu, D.; Zhou, C.; Zhang, M. Effect of Clay on Immiscible Morphology of Poly(Butylene Terephthalate)/Polyethylene Blend Nanocomposites. *J. Appl. Polym. Sci.* **2006**, *102*, 3628–3633, doi:10.1002/app.24088.
32. Yang, W.; Hu, Y.; Tai, Q.; Lu, H.; Song, L.; Yuen, R.K.K. Fire and Mechanical Performance of Nanoclay Reinforced Glass-Fiber/PBT Composites Containing Aluminum Hypophosphite Particles. *Compos. Part A Appl. Sci. Manuf.* **2011**, *42*, 794–800, doi:10.1016/j.compositesa.2011.03.009.
33. Khashkhozheva, R.R.; Zhansitov, A.A.; Khashirova, S.Y.; Mikitaev, A.K. The Development of Fireproof Composite Materials Based on Polybutylene Terephthalates. *Int. Polym. Sci. Technol.* **2016**, *43*, 47–52, doi:10.1177/0307174x1604300909.
34. Chalabi Tehran, A.; Shelesh-Nezhad, K.; Faraji Kalajahi, P.; Olad, A. A Study of the Effect of TPU and Clay Nanoparticles on the Mechanical Behavior of PBT-Based Nanocomposites. *Mech. Adv. Compos. Struct.* **2017**, *4*, 179–186, doi:10.22075/MACS.2016.499.
35. Chang, J.H.; An, Y.U.; Kim, S.J.; Im, S. Poly(Butylene Terephthalate)/Organoclay Nanocomposites Prepared by in Situ Interlayer Polymerization and Its Fiber (II). *Polymer (Guildf).* **2003**, *44*, 5655–5661, doi:10.1016/S0032-3861(03)00613-X.
36. Oburoğlu, N.; Ercan, N.; Durmus, A.; Kaşgöz, A. Effects of Filler Type on the Nonisothermal Crystallization Kinetics of Poly(Butylene Terephthalate) (PBT) Composites. *J. Appl. Polym. Sci.* **2012**, *123*, 77–91, doi:10.1002/app.34464.

37. Ślusarczyk, C.; Sieradzka, M.; Fabia, J.; Fryczkowski, R. Supermolecular Structure of Poly(Butylene Terephthalate) Fibers Formed with the Addition of Reduced Graphene Oxide. *Polymers (Basel).* **2020**, *12*, doi:10.3390/polym12071456.
38. Wu, F.; Yang, G. Poly(Butylene Terephthalate)/Organoclay Nanocomposites Prepared by in-Situ Bulk Polymerization with Cyclic Poly(Butylene Terephthalate). *Mater. Lett.* **2009**, *63*, 1686–1688, doi:10.1016/j.matlet.2009.05.011.
39. Hajibaba, A.; Masoomi, M.; Nazockdast, H. The Role of Hydrophilic Organoclay in Morphology Development of Poly(Butylene Terephthalate)/Polypropylene Blends. *High Perform. Polym.* **2016**, *28*, 85–95, doi:10.1177/0954008315571683.
40. Xiao, J.; Hu, Y.; Wang, Z.; Tang, Y.; Chen, Z.; Fan, W. Preparation and Characterization of Poly(Butylene Terephthalate) Nanocomposites from Thermally Stable Organic-Modified Montmorillonite. *Eur. Polym. J.* **2005**, *41*, 1030–1035, doi:10.1016/j.eurpolymj.2004.11.025.
41. Soudmand, B.H.; Shelesh-Nezhad, K.; Hassanifard, S. Toughness Evaluation of Poly(Butylene Terephthalate) Nanocomposites. *Theor. Appl. Fract. Mech.* **2020**, *108*, 102662, doi:10.1016/j.tafmec.2020.102662.
42. Delbem, M.F.; Valera, T.S.; Valenzuela-Diaz, F.R.; Demarquette, N.R. Modification of a Brazilian Smectite Clay with Different Quaternary Ammonium Salts. *Quim. Nova* **2010**, *33*, 309–315.
43. de Paiva, L.B.; Morales, A.R.; Valenzuela Díaz, F.R. Organoclays: Properties, Preparation and Applications. *Appl. Clay Sci.* **2008**, *42*, 8–24, doi:10.1016/j.clay.2008.02.006.
44. Celanese Celanex 1600a Datasheet Available online: http://www.matweb.com/search/datasheet t.aspx? matguid = b42d0ac49ce448f99238 bed352bb7496&ckck=1.
45. Deshpande, R.; Naik, G.; Chopra, S.; Deshmukh, K.A.; Deshmukh, A.D.; Peshwe, D.R. A Study on Mechanical Properties of PBT Nano-Composites Reinforced with Microwave Functionalized MWCNTs. *IOP Conf. Ser. Mater. Sci. Eng.* **2018**, *346*, doi:10.1088/1757-899X/346/1/012004.
46. Merah, N.; Mohamed, O. Nanoclay and Water Uptake Effects on Mechanical Properties of Unsaturated Polyester. *J. Nanomater.* **2019**, *2019*, doi:10.1155/2019/8130419.
47. Weng, Z.; Wang, J.; Senthil, T.; Wu, L. Mechanical and Thermal Properties of ABS/Montmorillonite Nanocomposites for Fused Deposition Modeling 3D Printing. *Mater. Des.* **2016**, *102*, 276–283, doi:10.1016/j.matdes.2016.04.045.
48. Baba-Ahmadi, S.B.; Hashemian, M.; Khosravi, M.; Khandan, A. An Experimental and Analytical Investigation of Novel Nanocomposite Reinforced with Nanoclay with Enhanced Properties for Low Velocity Impact Test. *J. Nanostructures* **2020**, *10*, 92–106, doi:10.22052/JNS.2020.01.011.
49. Sun, Y.; Mei, J.; Hu, H.; Ying, J.; Zhou, W.; Zhao, X.; Peng, S. In-Situ Polymerization of Exfoliated Structure PA6/Organo-Clay Nanocomposites. *Rev. Adv. Mater. Sci.* **2020**, *59*, 434–440, doi:10.1515/rams-2020-0038.
50. Pumchusak, J.; Thajina, N.; Keawsujai, W.; Chaiwan, P. Effect of Organo-Modified Montmorillonite Nanoclay on Mechanical, Thermo-Mechanical, and Thermal Properties of Carbon Fiber-Reinforced Phenolic Composites. *Polymers (Basel).* **2021**, *13*, 1–12, doi:10.3390/polym13050754.
51. Nirukhe, A.B.; Shertukde, V. V. Preparation and Characterization of Poly(Butylene Terephthalate) Nanocomposites with Various Organoclays. *J. Appl. Polym. Sci.* **2009**, *113*, 585–592, doi:10.1002/app.30112.
52. Zhang, Q.; Fu, Q.; Jiang, L.; Lei, Y. Preparation and Properties of Polypropylene/Montmorillonite Layered Nanocomposites. *Polym. Int.* **2000**, *49*, 1561–1564, doi:10.1002/1097-0126(200012)49:12<1561::aid-pi509>3.3.co;2-k.